JOURNAL OF SOLID STATE CHEMISTRY **107**, 43–57 (1993)

An X-Ray and Ultraviolet Photoemission Study of Vanadium Sulfides in the Series $VS_{1.0}$–$VS_{1.60}$

W. BENSCH AND R. SCHLÖGL

Institute for Inorganic Chemistry, University of Frankfurt, Niederurseler Hang, 60439 Frankfurt a.M., Germany

Received July 22, 1992; in revised form February 15, 1993; accepted February 17, 1993

A combined UPS and XPS study was performed on a series of structurally related vanadium sulfides of the NiAs type. The valence band spectra show systematic variations with the metal to sulfur ratio (1.0 to 1.6) such as an increase in the density of states with increasing sulfur content. These findings are discussed using structural information and band structure calculations of VS at the linear Muffin-Tin orbital (LMTO) level. The core level data of S 2*p*, S 2*s*, and V 2*p* exhibit much larger variations than expected from the valence band spectra indicating that the bonding interaction in the VS_6 octahedra vary with the elemental composition. The compounds contain a significant amount of dissolved atomic oxygen which forms oxides only after Ar ion bombardment. The presence of nonbonding oxygen was substantiated with XPS and IMR-MS thermal desorption spectroscopy. All data point to an alloy type electronic structure of these metalloid compounds resulting from a vanadium atom network with metallic contacts varying systematically in its topology with chemical composition.

1. Introduction

During the last decades both experimental and theoretical work have been performed to clarify the structural and physical properties of vanadium sulfides. Seven different crystal structures are known to exist in the composition range $VS_{1.0}$–$VS_{1.60}$. All are related to the hexagonal NiAs structure type. Additional structures have also been reported (*1*, *2*), but their existence is yet uncertain. They may be regarded as superstructures related to the NiAs type.

In general, the relationship between the NiAs structure and the crystal structures observed in the composition range mentioned above is as follows: in every second metal layer, which is perpendicular to the crystallographic *c*-axis, metal atoms are successively removed on going from $VS_{1.0}$ to $VS_{1.6}$ with the resulting vacancies being ordered in these structures. The vanadium atoms are always surrounded by six sulfur atoms leading to an octahedral environment.

A survey is given in Table I over the different phases and their homogeneity ranges.

All compounds exhibit short metal to metal distances. A metallic or semimetallic behavior is expected.

The arrangement of the metal atoms within the unit cell of VS(NiAs), VS(MnP), V_3S_4, and V_5S_8 is shown in Fig. 1. The main structural differences are due to the arrangement of the second nearest neighbors.

Therefore, we expect rather similar XPS core level spectra. The Madelung contribution to the chemical shift should be well comparable between all compounds.

The series $VS_{1.0}$–$VS_{1.60}$ offers, however, the unique possibility to study second order effects of non-next-neighbor interactions in photoemission. Furthermore, the change of the electronic structure as well as the changes of the features in the valence band

0022-4596/93 $5.00

TABLE I

The Homogeneity Range of Different V Sulfides Compiled from the Literature

VS (MnP-Type)	Ref.	VS (NiAs-type)	Ref.
$VS_{0.85}-VS_{1.05}$	*(23)*	$VS_{1.02}-VS_{1.22}$	*(26)*
$VS_{0.92}-VS_{1.06}$	*(24)*	$VS_{1.02}-VS_{1.16}$	*(27)*
$VS_{0.93}-VS_{1.06}$	*(2)*	$VS_{1.00}-VS_{1.16}$	*(1)*
? $-VS_{1.07}$	*(25)*	$VS_{1.02}-VS_{1.16}$	*(24)*
		$VS_{1.069}-VS_{1.18}$	(25)
V_7S_8 (hex)	**Ref.**	**V_7S_8 (mon)**	**Ref.**
$VS_{1.24}$	*(2)*	$VS_{1.16}$	*(33)*
V_3S_4	**Ref.**	**V_2S_3**	**Ref.**
$VS_{1.17}-VS_{1.55}$^{a}	*(1)*	$VS_{1.50}$	*(34)*
$VS_{1.18}-VS_{1.54}$	*(28)*	$VS_{1.50}$	*(35)*
$VS_{1.17}-VS_{1.54}$	*(27)*	$VS_{1.448}-VS_{1.515}$	*(32)*^{b}
$VS_{1.21}-VS_{1.51}$	*(2)*	$VS_{1.452}-VS_{1.532}$	*(32)*^{c}
$VS_{1.19}-VS_{1.58}$	*(29)*	$VS_{1.472}-VS_{1.529}$	*(32)*^{d}
$VS_{1.20}-VS_{1.54}$	*(30)*		
$VS_{1.18}-VS_{1.56}$	*(31)*		
$VS_{1.18}-$?	*(25)*		
$VS_{1.336}-VS_{1.431}$	*(32)*^{b}		
$VS_{1.334}-VS_{1.433}$	*(32)*^{c}		
$VS_{1.335}-VS_{1.455}$	*(32)*^{d}		
V_5S_8	**Ref.**		
$VS_{1.57}-VS_{1.64}$	*(30)*		
$VS_{1.55}-VS_{1.60}$	*(1)*		
$VS_{1.57}-VS_{1.68}$	*(31)*		
$VS_{1.547}-VS_{1.595}$	*(32)*^{b}		
$VS_{1.549}-VS_{1.586}$	*(32)*^{c}		

[a] $VS_{1.55}$ belongs to the V_3S_4 phase if quenched from 1073 K, while it belongs to the V_5S_8 phase if quenched from 1023 K (*1*, *32*). Complex phase relationships for hexagonal VS and V_3S_4 as a function of temperature are discussed in (*36*).

[b] Prepared at 650°C.

[c] Prepared at 700°C.

[d] Prepared at 750°C.

can be studied as a function of increasing S abundance.

The contribution presented here deals with X-ray photoelectron spectroscopy (XPS) and ultraviolet photoelectron spectroscopy (UPS) investigations performed at different temperatures.

Electronic band structure calculations were performed with the LMTO technique for both the NiAs and MnP type structure of VS to qualitatively compare the results with the experimental data. Besides a recently published extended Hückel molecular orbital calculation (*3*), it is the first self consistent field calculation of vanadium monosulfide with the MnP type structure. The detailed procedure as well as detailed results of the calculations will be published elsewhere (*4*).

One aim of this work is to characterize the nature of the metallic character in these compounds and to search for charge transfer effects using state selective high energy spectroscopy in order to complement the numerous low energy transport investigations.

2. Experimental

2.1. Preparations

Weighted amounts of vanadium powder and sulfur were placed in sealed and evacuated silica ampoules. Before using the silica ampoules were heated in HV to remove adsorbed water. The heat treatment for the different samples was performed according to Table II.

Due to the higher sulfur partial pressure, a lower temperature was chosen for the samples rich in sulfur in the first step. The products consist of microcrystalline gray to black powders.

2.2. X-ray Investigations

X-ray diffraction patterns were recorded with a Siemens D-500 diffractometer using monochromatized Cu*Kα* radiation. Before and after the measurement the alignment of the instrument was checked with silicon powder as a reference material. All diffraction patterns show only peaks which can be indexed on the basis of the homogenous sample. The lattice parameters were refined using the program LATCON (part of the X-RAY 76 system). The results are given in Table III. Lattice parameters for the dif-

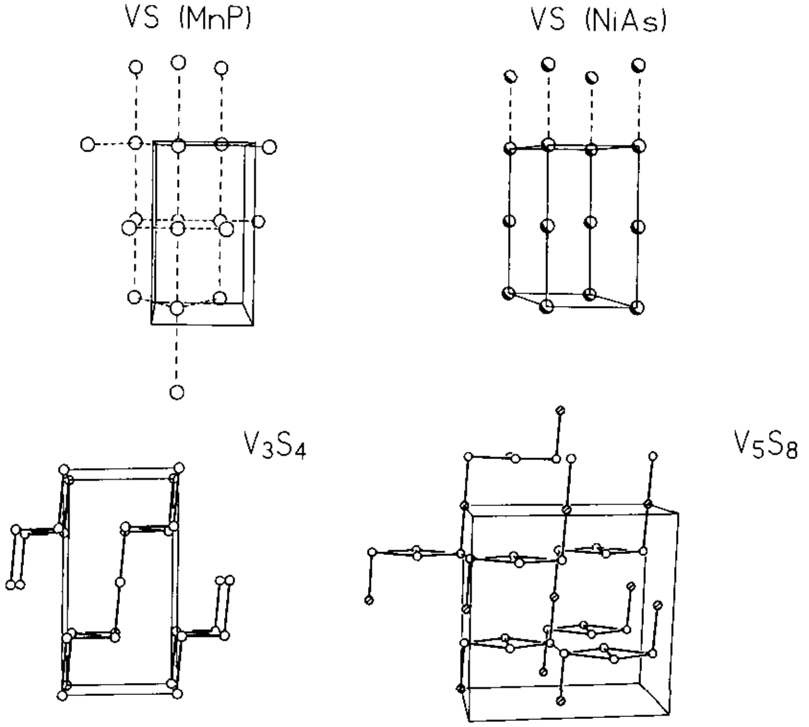

FIG. 1. The metal atom network in the vanadium sulfides VS (NiAs), VS (MnP), V_3S_4, and V_5S_8. The sulfur atoms are omitted for clarity.

ferent phases taken from the literature are given in Table IV.

2.3. *Photoemission*

The photoemission experiments were carried out in a Leybold-Heraeus ultrahigh vacuum environment with a base pressure of 2×10^{-10} mbar. The apparatus was equipped with a LHS 11N analyzer, magnesium X-ray source (nonmonochromated, 220 W), resonance lamp (He I, He II radiation) and sputtering facilities (Ar^+, 5 kV, 10 mA, 4×10^{-6} mbar, sputtering yield on gold 120 Å $(10\ \text{min})^{-1}$).

TABLE II

PREPARATION CONDITIONS FOR THE DIFFERENT VANADIUM SULFIDES

Compos.	Days	T (°C)	Days	T (°C)	gr	Days	T (°C)	co
$VS_{1.0}$	2	600	14	800	y	10	800	c
$VS_{1.33}$	4	500	14	800	y	14	800	c
$VS_{1.50}$	4	500	12	800	y	10	800	q
$VS_{1.60}$	2	480	10	650	y	16	800	c

Note. The "y" in column gr means grounded between the second and third step. "co," cooling: "c," cooling slowly to room temperature; "q," quenched in ice water.

Powder samples were placed in a stainless steel crucible mounted on a variable temperature (78–1000 K) introduction system. The binding energies are given relative to gold $4f_{7/2}$ (84.0 eV). Wide scan XPS spectra were obtained operating the analyzer with a constant retardation ratio of 4. High resolution XPS spectra were measured with the analyzer in a fixed transmission energy of 50 eV. Ultraviolet photoelectron (UP) spectra were obtained with a pass energy of 2 eV for He I (21.2 eV) and 20 eV for He II (40.8 eV).

3. Results

3.1. *Preparation of a Clean Surface*

The different vanadium sulfides investigated here were stored over a few weeks in

TABLE III

REFINED LATTICE PARAMETERS AND THE 2θ RANGE USED FOR THE REFINEMENT OF THE VANADIUM SULFIDES

VS (MnP type)	a = 3.307(1) Å	21.5° < 2θ < 85°
	b = 5.819(1) Å	
	c = 5.843(2) Å	
$VS_{1.33}$	a = 5.864(3) Å	15.6° < 2θ < 60°
	b = 3.283(1) Å	
	c = 11.360(5) Å	
	β = 92.08(5)°	
$VS_{1.50}$	a = 5.846(3) Å	15.5° < 2θ < 60°
	b = 3.280(1) Å	
	c = 11.367(6) Å	
	β = 91.68(4)°	
$VS_{1.60}$	a = 11.373(6) Å	15.0° < 2θ < 60°
	b = 6.648(2) Å	
	c = 11.298(4) Å	
	β = 91.46(4)°	

air. After introducing the samples into the spectrometer the composition of the surface of the compounds was quite different from the nominal composition indicated by a flat Fermi edge in the UPS as well as by a small S 2p core level peak at around 170 eV in the XPS, which is due to sulfur in vanadium sulfate or oxosulfate.

We used sputter cleaning, controlled by He I UP spectra and core level spectra showing the gradual appearance of the genuine surface of the compounds. Short sputtering intervals followed by spectroscopic examination proved to be less destructive than the equivalent sputtering dose applied in one step. After the sputtering sequence only one sample ($VS_{1.33}$) shows small amounts of sulfate (less than 5%) on the surface.

Nevertheless, the well-pronounced Fermi edge as well as the position of the main core levels let us conclude that the sputtering procedure has layed open the genuine sample surface. One interesting point of the core level spectra of all samples in the 530 eV b.e. region must be discussed in detail: all XPS core level spectra exhibit a relatively strong O 1*s* peak above 531 eV b.e. (see Table V). The O 1*s* core level spectra of $VS_{1.6}$ and $VS_{1.5}$ are displayed in Fig. 2. The O 1*s* peak does not disappear, even with sputtering times exceeding the data given here. In a first approximation one might conclude that the sample surfaces consist of vanadium oxides or sulfates/oxosulfates. But, as will be seen, the sulfur spectra gave no indication for appreciable amounts of sulfates/oxosulfates. Furthermore, the vanadium sulfates/oxosulfates are insulators, and therefore no Fermi edge should be observable (see Sections 3.2 and 3.3).

For vanadium oxides one expects an O 1*s* peak below 530 eV (529.6 eV for V_2O_5, 529.8 eV for VO_2 (*5*)). The O 1*s* b.e. of sputtered VO_x films is found to lie at about 530.4 eV. In addition, the observed O 1*s* peak in the different sulfides shows a clear temperature dependence (compare Table V and Fig. 2). Contrary to properties of oxides the oxygen species in various vanadium sulfide samples exhibit specific and pronounced changes upon cooling the samples to 78 K (dotted spectra in Fig. 2). In $VS_{1.60}$ some oxygen dissolves into the bulk of the sample. This reversible behavior requires a

TABLE IV

LATTICE PARAMETERS FOR DIFFERENT VANADIUM SULFIDES TAKEN FROM THE LITERATURE

	a [Å]	b [Å]	c [Å]	β	Ref.
VS (MnP)	5.854(7)	3.304(7)	5.820(2)	—	(*15*)
	5.822(2)	3.305(1)	5.859(2)	—	(*37*)
	5.860(1)	3.304(7)	5.826(5)	—	(*23*)
	3.305(2)	5.830(3)	5.856(4)	—	(*2*)
	5.825	3.310	5.854	—	(*1*)
$VS_{1.33}$	5.867(1)	3.282(1)	11.362(2)	92.05	(*2*)
	5.870	3.284	11.378	92.03	(*1*)
	5.850(2)	3.227(2)	11.349(4)	91.93	(*32*)[a]
	5.86	3.28	11.37	93.3	(*38*)
	5.831(1)	3.267(1)	11.317(2)	91.78(1)	(*39*)[b]
$VS_{1.50}$	5.816(1)	3.266(1)	11.310(2)	91.50	(*2*)
	5.828	3.276	11.366	91.73	(*1*)
	5.827(3)	3.275(2)	11.327(3)	91.69	(*32*)
$VS_{1.60}$	11.375(5)	6.648(2)	11.299(6)	91.50	(*2*)
	11.380	6.654	11.316	91.44	(*1*)
	11.37	6.65	11.29	91.31	(*40*)
	11.396(11)	6.645(7)	11.293(4)	91.45(6)	(*39*)

[a] Composition $VS_{1.422}$.

[b] Composition $VS_{1.47}$.

TABLE V

BINDING ENERGIES (eV) OF THE DIFFERENT CORE LEVELS IN THE VANADIUM SULFIDES

V/S		1.0	1.33	1.5	1.6
V $2p_{3/2}$	300 K	516.8	516.9	516.3	515.3
	78 K	517.1	516.3	516.3	515.1
FWHM		2.4	2.6	3.7	4.0
V $2p_{1/2}$	300 K	523.9	524.0	523.4	522.4
	78 K	524.2	523.4	523.4	522.3
V $3p$	300 K	41.8	41.6	41.2	40.1
	78 K	42.9	40.9	41.3	40.2
δ $2p$–$3p$	300 K	475.0	475.3	475.1	475.2
	78 K	474.2	475.4	475.0	474.9
S $2p$	300 K	162.9	162.2	163.0	162.8
	78 K	163.4	162.2	163.6	163.0
FWHM	300 K	3.1	3.0	3.4	3.1
	78 K	3.9	2.8	3.4	3.2
S $2s$	300 K	227.1	226.4	227.1	227.0
	78 K	227.4	226.2	227.5	227.1
FWHM	300 K	3.1	3.1	3.6	3.5
	78 K	3.9	3.2	3.7	3.5
δ $2s$–$2p$	300 K	64.2	64.2	64.1	64.2
	78 K	64.0	64.0	63.9	64.1
O $1s$	300 K	531.2	531.9	531.8	531.1
	78 K	531.8	530.8	533.0	531.3
FWHM	300 K	3.4	3.5	3.7	3.4
	78 K	3.6	3.6	4.4	3.6

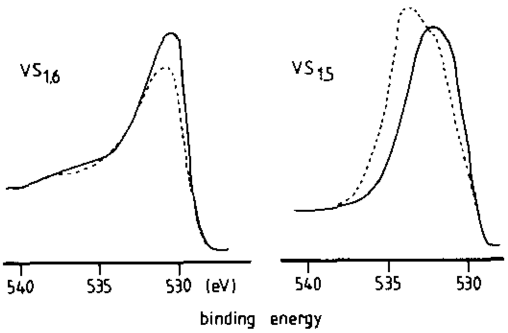

FIG. 2. XP spectra of the O $1s$ region of the two sulfides $VS_{1.5}$ and $VS_{1.6}$. The dotted peaks are recorded at 78 K. Note the change of the position and shape of the O $1s$ peak of $VS_{1.5}$.

change in the crystal structure of the material allowing more impurity atoms to be accommodated in the structural voids at low temperatures. This might be due to a change in the grain structure of the crystals modifying diffusion of the oxygen atoms. In $VS_{1.5}$ a significant shift to higher b.e. of most of the oxygen is observed upon cooling. The absolute b.e. of the O $1s$ reduces with increasing sulfur content with $VS_{1.0}$ being different from the other samples (see Table V). These changes can be interpreted as extra atomic-screening shifts indicating an increasing metallic character of the substrate with lower O $1s$ b.e.

The V-auger spectra (not displayed) are also quite different compared to those of vanadium oxides or vanadium metal (*5*). The possibility that the O $1s$ peak is caused by adsorbed H_2O can be excluded. It is well documented that the O $1s$ b.e. of adsorbed H_2O exhibits no shift with temperature. Furthermore, the assumption that at low temperatures the condensation of H_2O is responsible for the development of the O $1s$ at higher b.e.'s is unlikely as the surface abundance of oxygen is not increased at low temperature. In addition, water produces an intense characteristic valence band spectrum in the He II experiment featuring three intense bands which are all absent in our data. The He I and He II UP spectra at 78 K of all samples show a sharp Fermi edge. The condensatiaon of a H_2O layer should lead to insulating properties. Additionally, significant changes compared to the room temperature spectra should occur in the valence band region due to the emission of O $2p$ of the adsorbed H_2O.

All these points allow one to conclude that the oxygen is incorporated as an atomic species within the crystal structure establishing, however, no strong chemical bonds to the substrate but forming a solid solution of a nonmetal in a metallic matrix. This assumption is supported by investigations in the literature (*6–8*). All vanadium sulfides incorporate appreciable amounts of oxygen

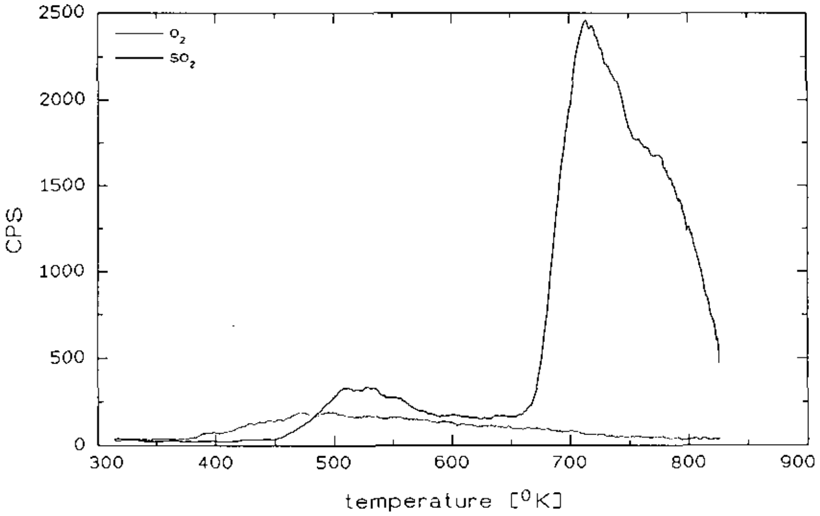

FIG. 3. IMR—MS spectrum of the compound V_3S_4 recorded in an Ar atomsphere. Note the two emission peaks of SO_2.

without significant changes in the crystal structures (*6*).

A variable composition of these solid solutions may well account for the differences in the lattice parameters published in the literature.

To further investigate the nature of the oxygen, mass spectrometry experiments have been performed with the IMR-MS technique (*9, 10*). In Fig. 3 the mass spectrum of $VS_{1.33}$ is displayed. Both the emission of oxygen and SO_2 was detected, the shape of the peaks and the emission temperatures being indicative for intrinsic oxygen. To exclude the possibility of a reaction of V oxides with V sulfides as the source for the observed oxygen emission additional mass spectrometry experiments with a mixture of V_2O_5 and VS_x were performed. It is noteworthy that no oxygen can be detected during the reaction. Furthermore, the SO_2 emission peak is clearly shifted to higher temperatures. A detailed study of this phenomenon is in progress and will be published elsewhere (*11*). These observations allowed us to conclude that the occurrence of oxygen in the samples is due to two effects. First, during the preparation of the sulfides oxygen is incorporated as a part of the crystal structure and secondly during the sputter cleaning the solid solution cannot be segregated into metal and oxide. From these experiments the amount of oxygen can be estimated to be in the bulk about 1 oxygen per 100 sulfur atoms. In the surface near regions this amount is increased due to the ease of diffusion as can be seen from the prepeak in the SO_2 emission of Fig. 3.

3.2. The He I UP and He II Room Temperature UP Spectra

The room temperature (300 K) He I and He II spectra of the different V sulfides are displayed in Figs. 4a and 4b, respectively.

All sulfides are metals but contrary to expectation the height of the Fermi edge increases with increasing the content of the nonmetal sulfur. It is noted that the height of the Fermi edge is significantly lower than in the pure V metal (compare Fig. 5). The work function of all sulfides was estimated from the He I cutoff and found to be 4.9 eV. This observation suggests that the sulfides are all poor metals and that the different bonding interactions between V–S and V–V are similar in the various sulfides.

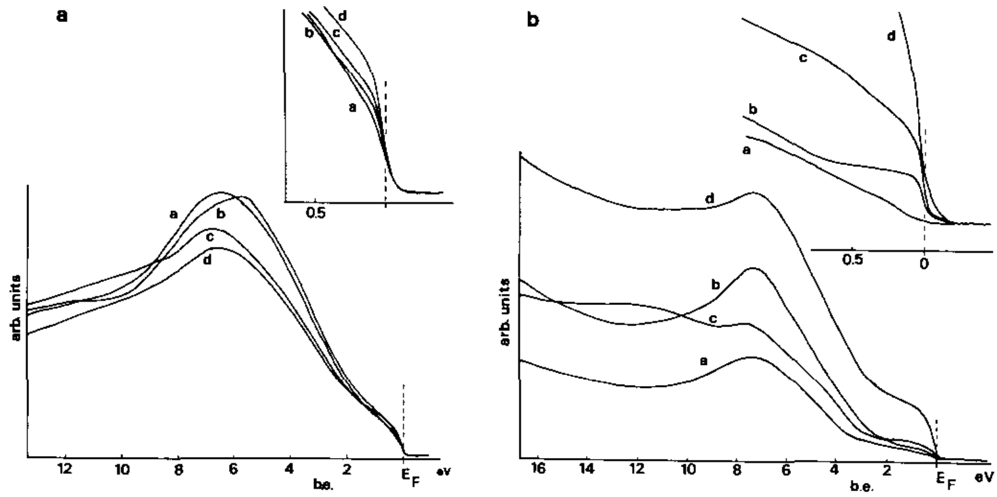

FIG. 4. (a): The He I UP spectra of VS (a), $VS_{1.33}$ (b), $VS_{1.5}$ (c), and $VS_{1.6}$ (d), recorded at 300 K. The inset shows an enlarged view of the region around E_F. (b): The He II UP spectra of VS (a), $VS_{1.33}$ (b), $VS_{1.5}$ (c), and $VS_{1.6}$ (d), recorded at 300 K. The inset shows an enlarged view of the region around E_F.

A comparison of the experimental valence band structure of $VS_{1.0}$ (MnP structure) with the calculated electronic band structure (LMTO level) is shown in Fig. 5. The width of the conduction band in the calculated DOS curve is about 2 eV and is in good agreement with the value from the experimental UPS data. The width is nearly identical with the width in pure V metal. The band structure calculation further reveals that some sulfur states also contribute to the conduction band. But the hybridization does not broaden this band. As can be seen from Fig. 5 (top) at about 2 eV below E_F a small gap of about 0.5 eV is calculated (see also (*12*)). The states near E_F are mainly due to V 3*d* contributions whereas the states below 2 eV are predominantly S 3*p* states.

XPS valence band spectra of hexagonal VS (*13*, *14*) show a relatively well resolved feature around 2 eV which is attributed to a pure V 3*d* band. The XPS study of orthorhombic VS gives no details about the valence band structure (*15*). In the sulfides investigated here the gap is not resolved despite the high resolution of the UP spectra. One reason may be the overlap of the conduction band with the He I β satellite of the main peaks. Furthermore, the LMTO calculations for $VS_{1.0}$ with the orthorhombic structure demonstrate that within the gap the density of states does not drop to zero but there are appreciable contributions from S 3*p* and V 3*d* states. Keeping in mind the different experimental cross sections for S and V states, the residual density of states may occur as exaggerated experimental intensity in the UP spectra so that the calculated gap is not reproduced.

No significant differences are observed in the DOS curves between the different modifications indicating that the changes of the vanadium sulfur bonding interactions have only a minor influence on the metallic character, which seems to be determined by the V–V interactions. Therefore, the small and not well resolved feature around 1 eV below E_F may be due to a band of predominantly metal *d* character.

With decreasing V abundance, the number of V–V contacts increases and the average V–V bond distance decreases. Consequently the height of the Fermi edge increases with increasing V : S ratio. It is noted that the feature around 6 eV below

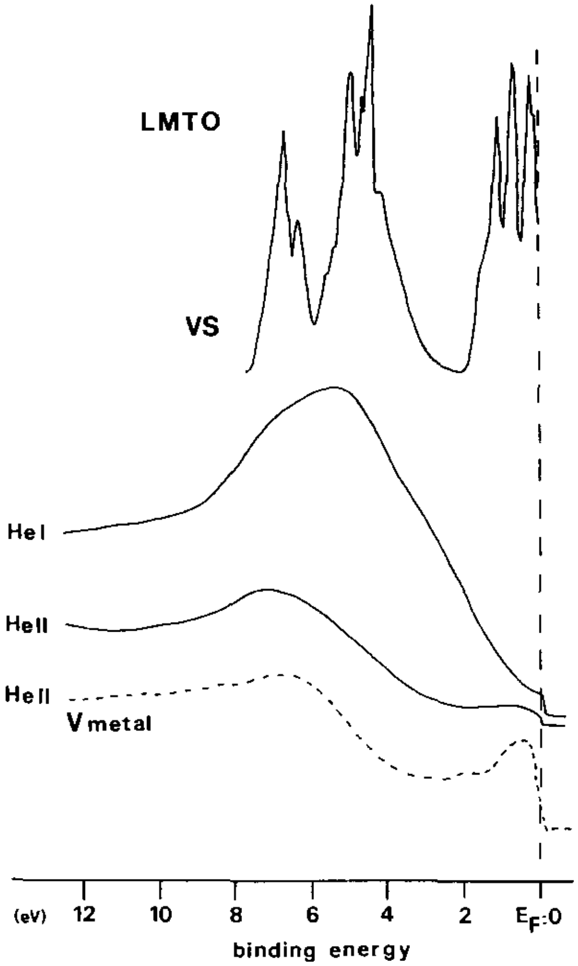

Fig. 5. The He I and He II valence band spectra of $VS_{1.0}$ with the MnP type structure. The He II UP spectrum of V metal is shown for comparison. In the upper part the resulting DOS of the LMTO calculations is displayed.

E_F of the monosulfide with the orthorhombic MnP structure (see Fig. 5) is quite different compared to that displayed in the literature for the hexagonal sulfide $VS_{1.09}$ (*13*). These significant differences are not reproduced by the band structure calculations for VS (NiAs) and VS (MnP). It is noted, however, that the peak shape in the literature spectrum is similar to that observed for VO_2 (*16*) and hence may be caused mainly by oxygen 2*p* states.

The variation of the intensity of the feature at 6 eV as a function of composition at different excitation energies is displayed in Fig. 6. Taking advantage of the cross section modulation of the He I and He II radiation it is demonstrated that the peak around 6 eV is mainly due to S states.

The LMTO calculations for VS in the MnP structure reveal a strong mixing of sulfur *p* with vanadium *s* and *p* states in the valence band. It is assumed, that such a high degree of rehybridization is also present in the other sulfides. Hence, the broad and not resolved feature in the binding energy range 2–8 eV can be interpreted as composed of sulfur *p* states with extensive broadening due to hybridization with vanadium *s* and *p* orbitals. Comparison of the VS spectra with that of pure elemental V (no oxygen seen in XPS) reveals an additional contribution of a valence band

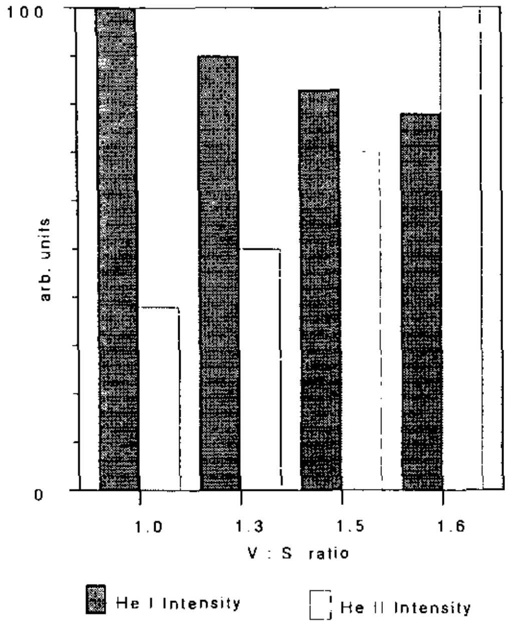

FIG. 6. The change of the intensity of the UP band maximum centered at around 6 eV b.e. as a function of composition. Note the different behavior for He I and He II radiation.

Auger transition to the intensity around 6 eV.

3.3. *The He I and He II UP Spectra at Low Temperatures (78 K)*

At 78 K the height of the Fermi edge exhibits the same trend as at 300 K except that $VS_{1.33}$ has a clearly higher Fermi edge than $VS_{1.50}$. No further significant changes are observed in the 78 K spectra of these two compounds.

Room temperature and low temperature UP spectra of $VS_{1.0}$ and $VS_{1.60}$ are displayed in Fig. 7. Comparing the He II UP spectra only small differences are observed. The height of the Fermi edge seems to be slightly higher at 78 K and the separation between the conduction band and the broad valence band is more pronounced at 78 K. These observations are explained with low temperature single crystal structural data which demonstrate that the V–S interactions are not significantly altered at 100 K. In contrast, striking changes occur within the vanadium metal network (*17*) which may account for the differences observed in the He II spectra at 78 K. Remarkable changes occur for $VS_{1.0}$ in both the He I and He II spectra. The broad valence band between about 2 and 10 eV below E_F reveals a less pronounced peak at about 7 eV. Furthermore, in the He I spectrum the valence band is clearly broader at 78 K and the intensity is enhanced. These observations indicate a change of the vanadium sulfur bonding interactions at 78 K. Unfortunately, no low temperature structural data are available which may help to explain the differences. It is known, however, that a number of compounds which crystallize in the orthorhombic MnP structure exhibit anisotropic expansion of the lattice parameters as function of temperature (*18*). Such an anisotropy may lead to a significant change of the V–S bonding interactions in $VS_{1.0}$.

3.4. *Sulfur 2p Core Level Spectra*

The 300 K S 2*p* core level spectra of the different sulfides are of similar shape and the peaks are asymmetric with respect to higher b.e. The widths of the S 2*p* core level lines indicate the presence of at least two sulfur species in the sulfides. The S $2p_{1/2}$ component is totally hidden under the broad peaks. The line shapes gave no hints to the number of different sites. Therefore, no attempts were made to fit different sulfur species under the observed core level peaks.

The binding energies of 162.2 to 163.0 eV (see Table V) are in the range observed for other covalent transition metal sulfides (see Table VI), but clearly below the value for sulfates. From the comparison of the observed b.e. with that of elemental sulfur only a low formal charge on the sulfur atoms can be expected. If a linear relationship between chemical shift and formal oxidation state is assumed the formal charge on the sulfur atoms is of about 1– in $VS_{1.33}$ and less than 1– in the other three sulfides. No systematic trend of the b.e. is observed when going from $VS_{1.0}$ to $VS_{1.6}$. At 78 K the formal

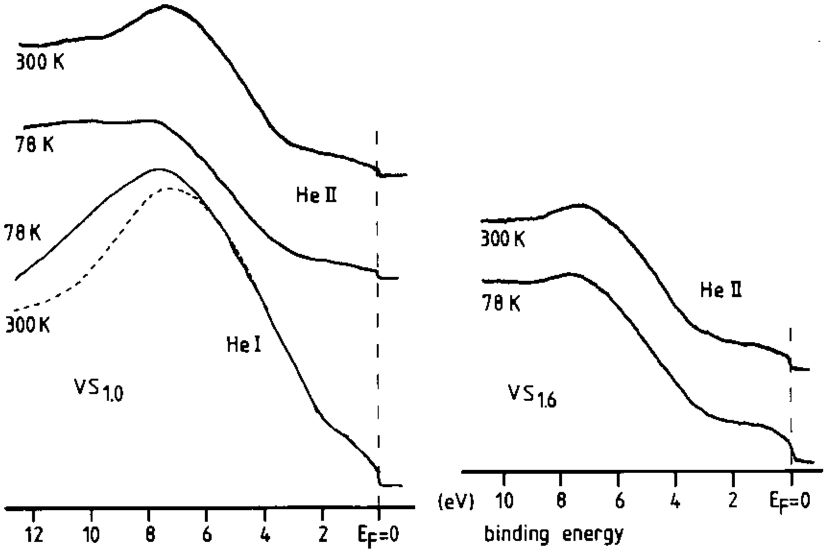

FIG. 7. He I and He II UP valence band spectra of $VS_{1.0}$ determined at 78 K and 300 K (left) and the He II UP spectra of $VS_{1.6}$ recorded at 78 and 300 K (right).

charge on the sulfur atoms in $VS_{1.0}$, $VS_{1.5}$, and $VS_{1.6}$ is lowered and now less than 1 −. The small changes in the b.e. may be caused by a contraction of the crystal axes at lower temperatures, and hence a different charge transfer from vanadium to sulfur, and vice versa, due to better orbital overlap. It should be noted here that these changes of the V–S bonding interactions are "hidden" under the broad and featureless valence band region in the UP spectra. Only small changes of the width and intensity of the valence band spectra are observed due to the low sensitivity of the low energy valence band data for small changes in the charge distribution characteristic for covalent compounds (see Section 3.2).

It is noteworthy, that only very small changes in b.e. and width of the S 2*p* core level are observed in $VS_{1.33}$. The variation of the crystal lattice parameters with temperature has a compensatory effect, thus leading to no appreciable changes in the 78 K spectrum.

The S 2*p* core level spectra as well as the V 2*p* spectra of $VS_{1.0}$ recorded at 300 K and 78 K are shown in Fig. 8. Whereas the 78 K S 2*p* core levels of $VS_{1.50}$ and $VS_{1.60}$ (not shown) shift only to slightly higher binding energies, both a shift and a line broadening are observed for $VS_{1.0}$ (compare Fig. 8). As discussed in the previous section an anisotropic contraction of the lattice parameters with temperature is assumed which may lead to pronounced changes of the V–S bonding interactions, especially a larger distribution of the V–S separations. These altered bonding properties may result in both a shift and a broadening of the S 2*p* core level. It should be stressed here that the changes in the S 2*p* region are in agreement with the observations discussed in Section 3.3.

3.5. Sulfur 2s Core Level Spectra

The 300 K S 2*s* core level spectra are displayed in Fig. 9. Additionally, the 78 K spectrum of $VS_{1.0}$ together with the b.e. of elemental sulfur are also shown. The S 2*s* line exhibits an asymmetric shape towards higher b.e. in all sulfides, not only at 300 K but also at 78 K. Since the 2*s* core level is a single line the observed asymmetry is highly indicative of several chemically in-

TABLE VI

BINDING ENERGIES (eV) FOR SULFUR AND VANADIUM IN DIFFERENT COMPOUNDS

Compound	S 2s	S 2p	δ (2s–2p)	Ref.
Cu_2S	226.6	162.2	64.0	(41)
CuS	225.9	161.3	64.6	(42)
$CuSO_4$	—	169.5		(42)
CuS		162.5		(43)
Cu_2S		161.77		(44)
CuS		161.8		(44)
CuV_2S_4		160.6		(44)
Ag_2S		162.3		(45)
$(NH_4)_3VS_4$		161.9		(45)
PbS	225.3	—		(46)
NiS	—	162.8		(47)
MnS	225.9	161.8	64.1	(48)
MnS		162.0		(15)
$NiPS_3$	227.3	163.9	63.4	(49)
Rh_2S_3	—	162.5		(50)
$SnMo_6S_8$	—	162.5		(51)
$VS_{1.04}$		162.3		(15)
$VS_{1.09}$	226.3	162.0	64.3	(13)
VS	225.5	161.6	63.9	(14)
CrS	225.8	161.7	64.1	(14)
TiS	226.0	162.3	63.7	(14)
V_2S_3		161.9		(52)
TiS		163.5		(15)
ScS		163.65		(15)
SrS		161.95		(15)
MgS		162.0		(15)
$ZnSO_4$	233.6	169.8	63.8	(53)
S (element)	227.9	163.7	64.2	(13)
Compound	V $2p_{3/2}$			
Li_3VO_4	517.5			(54)
V_2O_5	517.7			(54)
V_2O_5	516.6			(55)
V_2O_5	516.9			(45)
$VOSO_4$	515.9			(55)
VCl_3	515			(56)
VN	514.4			(57)
VP	512.6			(58)
$VS_{1.04}$	512.7			(15)
VS	513.4			(14)
$VS_{1.09}$	512.7			(13)
V_2S_5	514.4			(59)
VO_2	516.3			(5)
Tl_3VSe_4	518.0			(45)
$(NH_4)_3VS_4$	513.6			(45)
V	512.9			(5)
V	512.14			(60)
V	512.0			(61)

equivalent sites which are expected from the crystal structures discussed above.

A second possibility for the occurrence of the asymmetry may be an unresolved complex satellite structure due to different final states which lead to the asymmetry of the S 2s line. In such cases a fit of the data always yields unreasonable results. In addition, only for compounds with a high density of states at E_F (which the present compounds do not show; see Section 3.2) a pronounced asymmetry to the higher binding energy side is observed due to coupling of the core-hole with delocalized valence electrons (*19*).

At 300 K the binding energy for $VS_{1.0}$, $VS_{1.5}$, and $VS_{1.6}$ is about 0.9 eV lower than for elemental sulfur. Comparing this small shift with those observed for other transition metal sulfides (see Table VI) we again conclude that only a small negative charge is on the sulfur atoms. The S 2s b.e. of $VS_{1.33}$ is shifted by about 1.3 eV to lower b.e. relative to elemental S indicative for a more negative charge on the sulfur atom in this compound.

At 78 K the same trend as in the S 2p spectra is observed. The S 2s b.e. of $VS_{1.5}$ and $VS_{1.6}$ shifts to higher values, whereas that of $VS_{1.33}$ shows no shift. As can be seen from Fig. 9 the S 2s peak of $VS_{1.0}$ is clearly broadened compared with the 300 K spectrum, which may be explained by the arguments discussed in Section 3.4.

3.6. Vanadium 2p Region

The 300 K V 2p core level spectra are displayed in Fig. 10. As was pointed out in the experimental section the as-grown samples were covered by a layer consisting of vanadium sulfate/sulfite and/or vanadium oxide. During the sputter cleaning most of the oxygen bonded to the sulfur was removed. Nevertheless, the V 2p region clearly shows an O 1s peak located at around 531.5 eV (see Fig. 2). The b.e. is unusually high for a V oxide for which typical b.e.'s range from 529 to 530 eV (*20*). It is noted that the O 1s exhibits a reversible shift at

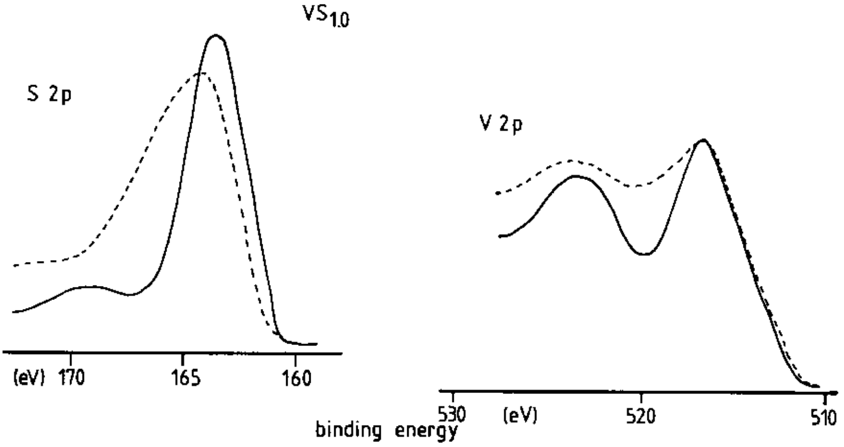

FIG. 8. The S $2p$ (left) and V $2p$ (right) core level XP spectra of $VS_{1.0}$ recorded at 300 K (full lines) and 78 K (dotted lines).

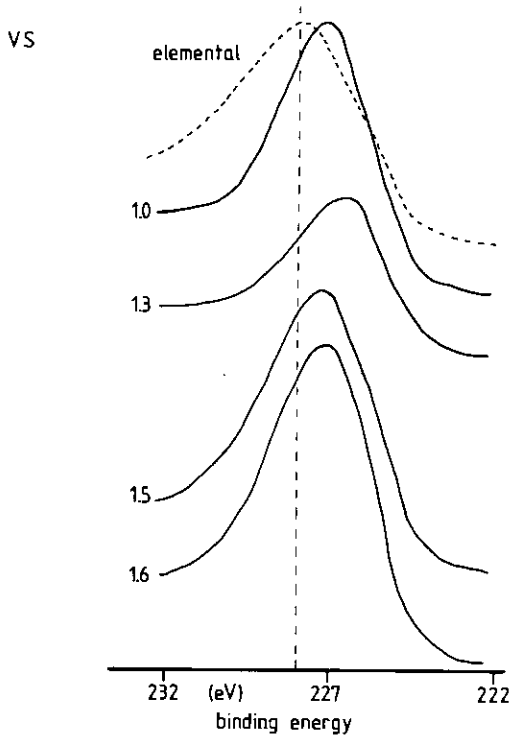

FIG. 9. The S $2s$ core level XP spectra of $VS_{1.0}$, $VS_{1.33}$, $VS_{1.5}$, and $VS_{1.6}$ determined at 300 K. For $VS_{1.0}$, the S $2s$ emission obtained at 78 K is also displayed (dotted line). The reference line represents the binding energy of elemental sulfur.

78 K, the direction of the shift depends on the V sulfide. In all cases the FWHM is clearly larger at 78 K suggesting the existence of more than one oxygen species.

One might argue that the sputter cleaning procedure leads to the formation of a mixture of VO_x and VS. But as was discussed in Sections 3.2 and 3.3 all samples show a sharp Fermi edge, the height being a function of the V : S ratio. To our knowledge V oxides are at 300 K insulators or semiconductors. Furthermore, the change of the position as well as the width of the V $2p_{3/2}$ core level in the series VS to $VS_{1.6}$ would suggest that more VO_x is present in the monosulfide than in $VS_{1.6}$. This is highly unlikely due to the fact that all samples were sputtered for the same time intervals. Additionally, it is more likely that the "open" system V_5S_8 is more easily oxidized than the dense VS with the MnP structure. Therefore, if the argon-ion etching procedure leads to the formation of V oxides, the VO_x abundance in V_5S_8 should be larger than in VS. The V $2p$ region around 515 eV shows two different signals. The V $2p$ signal at lower b.e. coincides well with the b.e. reported for V monosulfides (*13–15*) and the ternary compound $Tl_xV_6S_8$ (*21, 22*). The component at the higher b.e. may be due to vanadium suboxides which

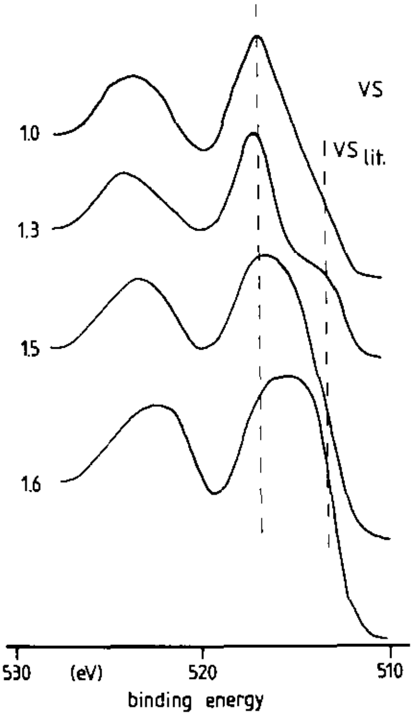

FIG. 10. The V 2*p* core level region of the XP spectra for the different sulfides. The line for VS taken from the literature is displayed for comparison. Note the change of the shape and width of the emission peaks.

have been "produced" during the sputter cleaning. This assumption is supported by the calculation of the surface elemental sample composition which in all sulfides yields a "ternary" oxosulfide with the formal composition VO_xS_y ($x \ll 1$; y near the expected value).

The FWHM of the V $2p_{3/2}$ peak seems to increase with increasing S content. This is consistent with the fact that the number of inequivalent V sites increases with increasing V : S ratio. But it is difficult to exactly evaluate the FWHM of this core level due to the high asymmetry and presence of a second peak caused by the V suboxides. Hence, no attempts have been made to fit the V $2p_{3/2}$ core level.

The change of the shape of the V 2*p* core level spectra is an indication for the alteration of the *d* electron density centered at the vanadium atoms. With decreasing *d* electron density the number and intensity of the possible final states decrease. Because it is difficult to separate the contribution of the V suboxides to the total V 2*p* core level shape a semiquantitative estimation of the formal *d* electron density is highly unreliable.

A comparison of the V 2*p* 300 K and 78 K spectra of $VS_{1.0}$ is shown in Fig. 8. Whereas the position of the peak exhibits no shift, the width and intensity are quite different at 78 K. Again, this variation is attributed to structural changes at low temperatures.

4. Conclusions

The metallic character of the vanadium sulfides in the series $VS_{1.0}$ to $VS_{1.60}$ was confirmed. HeI and HeII UP spectra demonstrate that with increasing V : S ratio the metallic behavior increases. This trend is in accordance with structural properties. With increasing sulfur abundance the number of V–V contacts increases. In all compounds the width of the conduction band is about 2 eV and the band is mainly due to V 3*d* states with a small admixture of S states. The hybridization does not broaden the conduction band. The valence band consists of S 2*p* states hybridized with vanadium *s* and *p* states. The width and shape of the valence band show no significant differences within the sulfide series. This observation suggests that the changes of the V–S bonding interactions do not remarkably influence the valence band.

Electronic band structure calculations performed for $VS_{1.0}$ with the orthorhombic MnP structure confirm the assignment of the different states derived from the HeI and HeII UP spectra. Low temperature UP spectra of $VS_{1.60}$ reveal an increase of the height of the Fermi edge. This change can satisfactorily be explained with low temperature structural data. Comparison of the 300 K and 78 K UP spectra of $VS_{1.0}$ exhibit pronounced changes of the valence band. These differences are attributed to changes of the V–S bonding properties at lower temperatures.

The S 2*p* and S 2*s* core level spectra both strongly suggest that the sulfur atoms carry a low negative charge. The estimated binding energies for these peaks are typical for transition metal sulfides. The pronounced asymmetry at the high b.e. side is indicative for more than one S species and/or for the highly covalent nature of the V–S bond leading to satellites. At 78 K the most significant changes are observed for the monosulfide. The position as well as the width of the peaks change significantly and these changes go hand in hand with the alterations in the valence band spectra. As mentioned above such differences must be related to changes of the crystal structure. The vanadium 2*p* core level spectra are complex and seem to be affected by artificially generated surface compounds during the sputter treatment. Nevertheless, the low b.e. component of V $2p_{3/2}$ demonstrates that the V atoms in all compounds have a low formal positive charge. It is noted that the high energy XP method is more sensitive to the small geometrical changes within the sulfide series than the UP valence band spectroscopy. The chemical information is comprised in the satellites which are due to many electron effects.

All compounds show an intense O 1*s* peak which can not be removed with a sputter cleaning procedure. The evaluated b.e. characteristic of a weakly charged atom and the absence of sulfate/sulfite contradicts the presence of common vanadium oxides and/or sulfates/sulfites. A reversible low temperature shift depending on the sulfide is observed. Hence, it is concluded that the oxygen is dissolved within the voids of the crystal structure. The emission of molecular oxygen upon heating the samples was further proved by mass spectrometry with the abundance being dependent on the preparation conditions and the actual composition (*11*).

In summary, the vanadium sulfides in the composition range $VS_{1.0}$ to $VS_{1.60}$ are metallic compounds of the alloy type. The phenomenon of oxygen dissolution is reminiscent of interstitial compounds characteristic of conventional metals. The chemical bonding in VS_x is highly anisotropic with low-dimensional metallic chains embedded in a covalently bonded V–S octahedral framework.

References

1. F. Gronvold, H. Haraldsen, B. Pedersen, and T. Tufte, *Rev. Chim. Miner.* **6,** 251 (1969).
2. A. B. deVries and F. Jellinek, *Rev. Chim. Miner.* **11,** 624 (1974).
3. J. Silvestre, W. Tremel, and R. Hoffmann, *J. Less-Common Met.* **116,** 113 (1986).
4. W. Bensch and H. Ebert, submitted for publication.
5. J. Kasperkiewicz, J. A. Kovacick, and D. Lichtman, *J. Electron. Spectrosc. Relat. Phenom.* **32,** 123 (1983).
6. J. Tudo, *Rev. Chim. Miner.* **2,** 53 (1965).
7. S. K. Basu, M. Wakihara, and M. Taniguchi, *Thermochim. Acta* **92,** 223 (1985).
8. S. K. Basu and M. Taniguchi, *J. Thermal. Anal.* **30,** 1129 (1985).
9. IMR-MS is a mild ionisation technique for small molecules which are reacted with a primary jet of low-energy noble gas (Kr) ions in a special octopole collision chamber.
10. W. Lindinger, *Phys. Rev. A* **7,** 328 (1973).
11. W. Bensch and H. Ochs, in preparation.
12. W. B. England, S. H. Liu, and H. W. Myron, *J. Chem. Phys.* **60,** 3760 (1974).
13. H. F. Franzen and G. Sawatzky, *J. Solid State Chem.* **15,** 229 (1975).
14. J. Gopalakrishnan, T. Murugesan, M. S. Hegde, and C. N. R. Rao, *J. Phys. C: Solid State Phys.* **12,** 5255 (1979).
15. H. F. Franzen, M. X. Umana, J. R. McCreary, and R. J. Thorn, *J. Solid State Chem.* **18,** 363 (1976).
16. C. Blaauw, F. Leenhouts, F. van der Woude, and G. A. Sawatzky, *J. Phys. C* **8,** 459 (1975).
17. W. Bensch and J. Koy, *Inorg. Chim. Acta,* **206,** 221 (1993).
18. K. Selte and A. Kjekshus, *Acta Chem. Scand.* **27,** 3195 (1973).
19. J. C. W. Folmer, and D. K. G. deBoer, *Solid State Commun.* **30,** 1135 (1981).
20. R. J. Colton, A. M. Guzman, and J. W. Rabalais, *J. Appl. Phys.* **49,** 409 (1978).
21. W. Bensch and R. Schlögl, *J. Less-Common Met.* **132,** 155 (1987).

22. W. Bensch, J. Koy, and M. Wesemann, *J. Alloys Compounds* **178,** 193 (1992).

23. H. F. Franzen and S. Westman, *Acta Chem. Scand.* **17,** 2353 (1963).

24. H. F. Franzen and T. J. Burger, *J. Chem. Phys.* **49,** 2268 (1968).

25. M. Nakano-Onoda and M. Nakahira, *J. Solid State Chem.* **30,** 283 (1979).

26. G.M. Loginov, *Russ. J. Inorg. Chem.* **6,** 133 (1961).

27. E. Hoschek and W. Klemm, *Z. Anorg. Allgem. Chem.* **242,** 49 (1939).

28. M. Saeki and M. Nakahira, "5th International Symposium High Purity Materials in Science and Technology," 144 ff., Dresden, May 5–9, 1980.

29. J. P. Delmaire, H. LeBusq, and F. Marion, *Compt. Rend.* **272,** 2144 (1971).

30. M. Saeki, M. Nakano, and M. Nakahira, *J. Cryst. Growth* **24/25,** 154 (1974).

31. Y. Oka, K. Kosuge, and S. Kachi, *J. Solid State Chem.* **23,** 11 (1978).

32. M. Wakihara, T. Uchida, and M. Taniguchi, *Met. Trans. B* **9,** 29 (1978).

33. S. Brunie, M. Chevreton, and J. M. Kauffmann, *Mater. Res. Bull.* **7,** 253 (1972).

34. H. Hahn and C. Lorent, *Angew. Chem.* **68,** 523 (1956).

35. T. A. Hewston and B. L. Chamberland, *Mater. Res. Bull.* **19,** 423 (1984).

36. T. Uchida, H. Hinode, M. Wakihara, and M. Taniguchi, *Met. Trans. B* **12,** 71 (1981).

37. H. F. Franzen and G. A. Wiegers, *J. Solid State Chem.* **13,** 114 (1975).

38. M. Chevreton and A. Sapet, *Compt. Rend.* **261,** 928 (1965).

39. I. Kawada, M. Nakano-Onoda, M. Ishii, M. Saeki, and M. Nakahira, *J. Solid State Chem.* **15,** 246 (1975).

40. S. Brunie and M. Chevreton, *Compt. Rend.* **258,** 5847 (1964).

41. B. R. Strohmeier, D. E. Leyden, R. S. Field, and D. M. Hercules, *J. Catal.* **94,** 514 (1985).

42. V. G. Bhide, S. Salkalachen, A. C. Rostagi, C. N. R. Rao, and M. S. Hedge, *J. Phys. D.* **14,** 1647 (1981).

43. D. Brion, *Appl. Surf. Sci.* **5,** 133 (1980).

44. J. C. W. Folmer and F. Jellinek, *J. Less-Common Met.* **76,** 153 (1980).

45. A. Müller, Ch. K. Jorgensen, and E. Diemann, *Z. Anorg. Allgem. Chem.* **391,** 38 (1972).

46. D. S. Zingg and D. M. Hercules, *J. Phys. Chem.* **82,** 1992 (1978).

47. C. D. Wagner and J. A. Taylor, *J. Electron. Spectrosc. Relat. Phenom.* **20,** 83 (1980).

48. B. R. Strohmeier and D. M. Hercules, *J. Phys. Chem.* **88,** 4922 (1984).

49. F. S. Khumalo, C. G. Olsen, J. W. Anderegg, and D. W. Lynch, *Chem. Phys.* **65,** 289 (1982).

50. K. E. Givens and J. G. Dillard, *J. Catal.* **86,** 108 (1984).

51. K. F. McCarty, J. W. Anderegg, and G. L. Schrader, *J. Catal.* **93,** 375 (1985).

52. D. Lichtman, J. H. Craig, Jr., V. Sailer, and M. Drinkwine, *Appl. Surf. Sci.* **7,** 325 (1981).

53. B. R. Strohmeier and D. M. Hercules, *J. Catal.* **86,** 244 (1984).

54. V. I. Nefedov, M. N. Firsov, and I. S. Shaplygin, *J. Electron. Spectrosc. Relat. Phenom.* **26,** 65 (1982).

55. R. Larson, B. Folkesson, and G. Schoen, *Chem. Scr.* **3,** 88 (1973).

56. B. Horvath, J. Strutz, J. Geyer-Lippmann, and E. G. Horvath, *Z. Anorg. Allgem. Chem.* **483,** 181 (1981).

57. M. Romand and M. Roubin, *Analusis* **4,** 309 (1976).

58. C. E. Myers, H. F. Franzen, and J. W. Anderegg, *Inorg. Chem.* **24,** 1822 (1985).

59. E. Diemann and A. Müller, *Z. Anorg. Allgem. Chem.* **444,** 981 (1978).

60. A. Lebugle, U. Axelsson, R. Nyholm, and N. Martensson, *Phys. Scr.* **23,** 825 (1981).

61. J. C. Fuggle and N. Martensson, *J. Electron. Spectrosc. Relat. Phenom.* **21,** 275 (1980).